

# PG 1700+518 Revisited: Adaptive Optics Imaging and a Revised Starburst Age for the Companion

Alan Stockton<sup>1</sup>, Gabriela Canalizo<sup>1</sup>, and Laird M. Close<sup>2</sup>

Institute for Astronomy, University of Hawaii, 2680 Woodlawn Drive, Honolulu, HI 96822

## ABSTRACT

We present the results of adaptive-optics imaging of the  $z = 0.2923$  QSO PG 1700+518 in the  $J$  and  $H$  bands. The extension to the north of the QSO is clearly seen to be a discrete companion with a well-defined tidal tail, rather than a feature associated with the host galaxy of PG 1700+518 itself. On the other hand, an extension to the southwest of the QSO (seen best in deeper, but lower-resolution, optical images) does likely comprise tidal material from the host galaxy. The SED derived from images in  $J$ ,  $H$ , and two non-standard optical bands indicates the presence of dust intermixed with the stellar component. We use our previously reported Keck spectrum of the companion, the SED found from the imaging data, and updated spectral-synthesis models to constrain the stellar populations in the companion and to redetermine the age of the starburst. While our best-fit age of 0.085 Gyr is nearly the same as our earlier determination, the fit of the new models is considerably better. This age is found to be remarkably robust with respect to different assumptions about the nature of the older stellar component and the effects of dust.

*Subject headings:* galaxies: interactions, quasars: individual (PG 1700+518)

## 1. Introduction

PG 1700+518 ( $z = 0.2923$ ), one of the more luminous low-redshift QSOs, shows a bright, arc-like structure extending about  $2''$  to the north of the QSO (Hutchings, Neff, & Gower 1992; Stickel *et al.* 1995). We recently presented a spectrum of this extension, showing that it is dominated in the optical by a stellar population  $\sim 10^8$  years old (Canalizo & Stockton 1997; hereinafter Paper 1). We argued that it is plausible that this starburst and the QSO activity were both triggered by a recent interaction, and that spectroscopic dating of starbursts in QSO hosts

---

<sup>1</sup>Visiting Astronomer, W.M. Keck Observatory, jointly operated by the California Institute of Technology and the University of California.

<sup>2</sup>Visiting Astronomer, Canada-France-Hawaii Telescope, operated by the National Research Council of Canada, the Centre National de la Recherche Scientifique de France, and the University of Hawaii.

and strongly interacting companions could lead to the development of an empirical evolutionary sequence for QSOs. From the imaging data we had on PG 1700+518 at that time, we were unsure whether the extension was a companion galaxy or a feature associated with the host galaxy of the QSO. Here we describe the results of adaptive-optics (AO) imaging and show that the object is indeed a discrete companion galaxy undergoing strong interaction with the QSO host. We combine these data with previous imaging in two optical bandpasses to give a spectral-energy distribution (SED) from  $0.42 \mu\text{m}$  to  $1.28 \mu\text{m}$  in the rest frame in order to place additional constraints on the stellar populations. We then use these constraints and fits of new spectral synthesis models to the Keck LRIS spectrum to obtain a more reliable age for the post-starburst component.

## 2. Observations and Data Reduction

The AO observations of PG 1700+518 were obtained at the f/36 focus of the Canada-France-Hawaii Telescope (CFHT) on 1997 July 14 and 15 (UT) with the University of Hawaii AO system (Roddier, Northcott, & Graves 1991; Roddier *et al.* 1994). In the version of the system used for these observations, an image of the telescope primary was formed on a 13-element deformable mirror that compensated the wavefront aberrations. Light shortwards of  $\sim 1 \mu\text{m}$  was sent by a beamsplitter to a membrane mirror, which was driven at 2.6 kHz to image extrafocal images on both sides of focus onto an avalanche-photodiode array. Corrections for the wavefront errors derived from the difference of these extrafocal images were sent to the deformable bimorph mirror, which was updated at 1.3 kHz. An important feature of this curvature-sensing AO system is that the correction level degrades gracefully for fainter guide sources. To approach the full correction of which the system is capable, a star with  $R \sim 12$  is required. We used the QSO itself, with  $R \sim 15.5$ , for wavefront sensing; nevertheless, we still achieved a substantial degree of correction.

Light longwards of  $\sim 1 \mu\text{m}$  was passed by the beamsplitter to the  $1024 \times 1024$  QUIRC (HgCdTe) infrared camera (Hodapp *et al.* 1996), which gave an image scale of  $0''.035 \text{ pixel}^{-1}$  and a field of  $36''$ . All of the exposures were 300 s; we obtained 22 exposures in the  $J$ -band and 18 exposures in the  $H$ -band. For both filter sequences, the telescope was offset to a new position after every two images in order to allow the construction of an object-free sky frame. Flat-field images were obtained from twilight-sky exposures. Flux calibration was obtained from observations of the standard G93-48 (Casali & Hawarden 1992).

The images were reduced by an iterative procedure. A bad-pixel mask was made by combining hot pixels from dark frames and dead pixels from flat-field frames. Subsets of the dark-subtracted raw images of the target, corresponding to  $\sim 2000$  s integration time each, were normalized by their median sky values and median averaged to obtain sky frames (bad pixels being excluded from the calculation). The sky frames were then scaled to the sky value of each raw frame and subtracted, and the residuals were divided by the flat-field frame. These were then registered to the nearest pixel and median-averaged. After a slight smoothing, this rough combined frame was used to generate object masks for each frame, which were combined with the bad-pixel mask. The

process was then repeated to generate better sky frames, better offsets for the alignment, and a new combined image. This image was used to replace bad pixels in each flattened frame with the median of the other frames, so that the bad pixels would not skew the centering algorithms used to calculate the offsets. The final combined image was a straight average of the corrected, sub-pixel-registered, flat-fielded frames, using a sigma-clipping algorithm in addition to the bad-pixel mask to eliminate deviant pixel values. The intrinsic FWHM of the QSO in the summed  $J$ -band and  $H$ -band images are  $0''.32$  and  $0''.28$ , respectively, while the uncorrected image quality averaged  $\sim 0''.8$  at  $J$  and  $\sim 0''.7$  at  $H$ .

It was not possible to obtain an adequate separate measure of the point-spread-function (PSF), so we had to generate a model of the PSF from the QSO itself. An image of a star obtained the same night with the same observing setup was found to have a high degree of symmetry, so we assume elliptical symmetry for the model. This procedure has the disadvantage that it will prevent the recovery of elliptically-symmetric components of the QSO host galaxy, but it does allow us to detect and carry out deconvolutions of non-symmetric components. We used the STSDAS tasks *ellipse* and *bmodel* to create a PSF model from modified images of the QSO, in which we replaced portions of the profile near the northern extension with the corresponding portions of the southern part of the profile, rotated  $180^\circ$  about the center. The elliptical fitting routine takes a median average along each elliptical isophote, reducing sensitivity to azimuthal structure and deviant pixels.

We used this model PSF for both straight PSF subtraction and deconvolution with *plucy* (Hook *et al.* 1994), which performs a two-channel deconvolution, using the standard Richardson-Lucy algorithm for designated point sources and a Richardson-Lucy procedure modified by the inclusion of an entropy term for the remainder of the image. The major advantage of *plucy* for detecting structure around QSOs is that the Richardson-Lucy non-negativity criterion is enforced against the background component instead of against a fixed zero point, and this feature eliminates the ringing problem typically seen around point sources in standard Richardson-Lucy restorations.

In order to determine the SED of the companion, we use optical images from Stockton, Ridgway, & Kellogg (1998), as well as the AO  $J$  and  $H$  images. We first convolve the images with appropriate Gaussian profiles to bring stellar objects to the same FWHM as those in the poorest of the images ( $0''.86$ ). We then subtract similarly convolved PSFs from the QSO profiles and do the photometry on these subtracted images.

### 3. Results and Discussion

#### 3.1. The Morphology of the Companion Galaxy

The AO images of PG 1700+518 are shown in Fig. 1, in original, PSF-subtracted, and *plucy*-restored versions. The extension to the north of the QSO, which has the appearance of an

arc-like or “boomerang” shape in the best previous ground-based images (Hutchings & Neff 1992; Stickel *et al.* 1995; Paper 1), retains that general appearance in our higher-resolution images, but it now also shows discrete condensations within this overall structure. It is also clearly a separate companion galaxy: there is a rather abrupt dropoff in surface brightness just south of the brightest condensation, whereas we would expect to see more continuity with the inner regions if this were a tail associated with the host galaxy. Such a connection should stand out in spite of our using the QSO to model the PSF, since we expect to be sensitive to any non-elliptically-symmetric features. The companion, though distinct, is apparently in the process of merging with the QSO host galaxy. The main features of the companion are consistent between the  $J$  and  $H$  images and must be real. The bright condensation  $a$  is probably the nucleus of the companion. The apparent tidal tail, curving to the north and east, contains another condensation,  $b$ , which may be a bright star-forming region or even a dwarf galaxy forming from the tidal debris (*e.g.*, Duc & Mirabel 1994; Hunsberger, Charlton, & Zaritsky 1996). The nature of features at lower surface brightnesses is less certain because of the effect of noise on the deconvolution. There is clearly material to the east of  $a$ , looking like another condensation in the  $J$  image, but more like an arc in the  $H$  image. The peak to the south of  $a$  on the  $J$  image is apparently an artifact of inadequacies in the PSF model, but there is some evidence in these images for bridge-like material between the companion and the QSO.

If most of the luminous material north of the QSO is associated with the companion, is there any evidence for tidal debris from the QSO host? Stickel *et al.* 1995 noted a possible faint extension to the SW of the QSO, which can also be seen in Fig. 2 of Paper 1. Here we show this feature in two optical bandpasses in Fig. 2, where we have slightly oversubtracted the wings of the PSF profile to show the SW extension more clearly. We suggest that this is likely a counter-tidal feature from the QSO host. The inner, higher-surface-brightness contours of the host galaxy appear to be aligned nearly E–W (Paper 1).

As we were completing this *Letter*, we were informed that Hines *et al.* 1998 had obtained a Hubble Space Telescope NICMOS image of PG 1700+518. They also conclude that the extension to the N is a companion, but they see what we have described as a tidal tail rather as part of a ring.

### 3.2. The SED of the Companion and the Age of the Starburst

In Paper 1, we presented a spectrum of the companion, corrected for contamination from the QSO. We modeled the SED as a superposition of two simple stellar populations (instantaneous bursts). Our age estimates, based on a  $\chi^2$  fit of the Bruzual & Charlot (1993) models to the spectrum of the companion, gave 0.09 (+0.04, –0.03) Gyr and 12.25 Gyr, respectively, for the two components.

Two recent developments encourage us to try to refine these estimates: better models

are now available (Bruzual & Charlot 1998), and we now have images in bandpasses covering a wide spectral range, which can additionally constrain the stellar populations. We use the same Keck Low-Resolution Imaging Spectrograph (LRIS) data from Paper 1. Because we need fairly high resolution for detailed fitting to features in the spectrum, we restrict ourselves to the solar-metallicity spectral-synthesis models based on the Gunn & Stryker (1983) and Jacoby, Hunter, & Christian (1984) spectra. We first discuss fits to the Keck LRIS spectrophotometry, considered in isolation; then we show how the models must be modified to take into account the SED over a wider wavelength region. Although the fit to the spectrum shown in Fig. 3 is from our final model, it is typical of the quality of fit we find for other models we discuss here.

If we try a similar approach to that of Paper 1, using only simple stellar populations from the newer models (Bruzual & Charlot 1998), we obtain nearly the same age for the younger population (0.10 Gyr), but a much younger age for the older population (1.8 Gyr). While this new model fits the Keck spectrum much better than did the model given in Paper 1, and we could no doubt improve the fit even more by adding a third, older population, the morphological evidence suggests another approach. The presence of a strong tidal tail indicates a dominant, pre-existing disk component, and the evidence for recent star formation indicates a gas-rich system. Such a galaxy would be expected to have been forming stars over the entire lifetime of the disk. We therefore consider another range of models: those in which there has been an exponentially-decaying rate of star formation on which is superposed a single recent starburst. Specifically, we assume that the younger population can be modelled as a burst (there is no appreciable difference in this case whether the burst is taken to be instantaneous or has a finite duration of several Myr) and that the older population has an exponentially-decaying star formation beginning 10 Gyr ago. We find that the age of the younger population and the quality of the fit are insensitive to the decay rate of star formation in the older component over a reasonable range (time constants  $\sim 3\text{--}10$  Gyr), but that we cannot get as good fits to the observed spectrum for either an old instantaneous burst or a constant star-formation rate. For definiteness, we assume an exponential time constant of 5 Gyr. Considering only the Keck spectrophotometry, we find the best  $\chi^2$  fit by combining this underlying population with a starburst with an age of 114 Myr. We now deal with additional constraints from the SED at longer wavelengths.

We determine the SED of the companion over a rest-frame range from  $0.42\ \mu\text{m}$  to  $1.28\ \mu\text{m}$  from the AO *J* and *H*-band images and images in two non-standard optical bands centered at 5442 and 7248 Å, with FWHM of 1002 and 1260 Å, respectively (see Fig. 2; these bandpasses have been designed to avoid strong emission lines at the redshift of PG 1700+518). Figure 4 shows the flux densities in these four filters for a  $1''$  diameter aperture centered  $0''.4$  E and  $2''.3$  N of the QSO. This region is far enough from the QSO that the photometry should not be very sensitive to the chosen scaling or other errors in the PSF subtraction process. While it does not exactly coincide with the region covered by the Keck LRIS spectrum, and there could be small differences in the two SEDs, we attempt to find a model that will fit both. We have explored a wide variety of SEDs involving superpositions of both simple and composite stellar populations based on the Bruzual & Charlot

(1998) models; none of these gives a satisfactory fit both to the Keck LRIS spectrum and to the wide-band SED. A pure old population comes moderately close to matching the overall SED, but it fails completely to reproduce either the strong Balmer absorption spectrum or the continuum shape of the restframe UV—blue spectrum. On the other hand, the “reddest” reasonable model we can find that adequately fits the Keck spectrum and the optical photometry falls well below the  $J$  and  $H$  points (see Fig. 4). Even this latter model is rather unphysical, comprising a pure young population (to fit the UV—blue spectrum) and a pure old stellar population (to attempt to fit the IR photometry), with nothing in between; however, the addition of any intermediate-age component only makes the fit worse.

Clearly one plausible way to raise the relative flux at longer wavelengths while retaining an early-type spectrum at shorter wavelengths is to include some sort of reddening due to dust. However, simply applying a Galactic reddening law (*i.e.*, assuming a dust screen between the object and the observer) is neither appropriate nor very effective. Screen-like reddening sufficient to force a fit to the overall SED results in very strong variation in extinction across the range of the Keck spectral fit, making it difficult to fit simultaneously the lines and continuum. One needs a means of effecting a substantial reddening of the IR flux with respect to the optical flux without changing the slope in the UV—blue region too much. Witt, Thronson, & Capuano (1992) have shown that dust distributions that are more-or-less coextensive with the stellar distribution, in addition to being more realistic, can provide exactly this sort of reddening. Such models differ from the standard reddening law (due to intervening dust) in two main respects: (1) some of the blue light removed along the sightline is compensated by scattering of blue light emitted in other directions into the line of sight, and (2) optical depth effects ensure that most of the light appearing at short wavelengths has suffered little extinction, while, at longer wavelengths, a larger portion of the total stellar distribution contributes to the emergent flux. We have used the family of “dusty galaxy” models calculated by Witt *et al.* (1992) to produce sets of modified Bruzual & Charlot (1998) models. The dust and the stars are both assumed to have constant density within a sphere, and the only variable is the optical depth to the center at a specific wavelength. While these models are highly artificial, they are sufficient to show the general nature of the reddening due to embedded dust, and they give us a good fit to both the LRIS spectrophotometry and the wide-band SED. We have included in Fig. 4 the model we have found to give the best fit to both the Keck spectral data and the overall SED. This same model is shown in Fig. 3, both as fit to the Keck spectrum and as individual components: the starburst, represented by an 85-Myr-old instantaneous burst, and the underlying population having star formation beginning 10 Gyr ago and exponentially decaying with a time constant of 5 Gyr. Both components are reddened by the curve given by the Witt *et al.* (1992) “dusty galaxy” model with a  $V$ -band central optical depth of 6.

The fit of the model to the Keck LRIS spectrophotometry (Fig. 3) is remarkably good, reproducing most individual features as well as the continuum slopes quite accurately. We can account for most of the deviations. Poor fits to  $H\beta$  (and, to a lesser extent,  $H\gamma$ ) absorption are

due to distortion of these profiles by general emission around the QSO not specifically associated with the companion: there is both a positive component and a negative component (at a higher velocity, from the region on the opposite side of the QSO that was used to subtract off scattered QSO light; see Paper 1 for details). Similarly, the excess peak near 3868 Å is due to [Ne III] emission. The broad dip between 4500 and 4600 Å is due to excess subtraction of Fe II emission, which is apparently spatially variable (Paper 1). We have found that we can improve the fit of the Ca II *K* line by including a secondary burst  $\sim 2$  Gyr ago, which may be evidence for a previous close passage of the companion, but this evidence alone is slender enough that we have chosen not to include this added complexity to the model. The only significant discrepancy that we cannot explain is the poor fit to H10  $\lambda 3798$ ; this may simply be due to a glitch in our observed spectrum.

### 3.3. Towards an Evolutionary Sequence for QSOs

Although the SED model we have presented is the best fit we have found to the data, subject to the constraints of simplicity and astrophysical reasonableness that we have chosen, we can find other models that fit nearly as well. However, in exploring various models, we have found that, for reasonably plausible combinations of young and old stellar populations and reddening curves (*i.e.*, those that come close to fitting both the LRIS spectrophotometry and the overall SED), there is very little spread in the age of the young population. We consistently obtain ages in the range from 75 to 100 Myr, and we believe that this is a reasonable estimate of the uncertainty in our determination, subject only to any remaining uncertainty in the Bruzual & Charlot (1998) models themselves. We regard this robustness in the age determination as a hopeful sign for our ongoing efforts to develop an age sequence for triggering events for QSOs lying in the transition region between ultraluminous IR galaxies and the classical QSO population in the far-IR two-color diagram (Paper 1; Canalizo & Stockton 1998; Stockton 1998).

This enthusiasm is only slightly dampened by the fact that the AO imaging shows clearly that our age determination is for the interacting companion to PG 1700+518, rather than for the host galaxy itself. Obtaining similar quality spectrophotometry for the extension of the host galaxy to the SW, which is both considerably fainter and closer to the QSO, would be extremely difficult. Nevertheless, its colors appear to be quite similar to those of the companion, and models of starbursts in interacting pairs (*e.g.*, Mihos & Herquist 1996) indicate that star formation peaks at times of closest passage in both participants. The projected  $\sim 2''$  ( $\approx 7$  kpc) separation between the QSO and companion and the projected  $\sim 5$  kpc tail length of the companion are entirely consistent with a close passage 85 Myr ago, if projection factors are  $\sim 0.5$  and mutual velocities are  $\sim 150$  km s $^{-1}$ . We therefore believe that the age of starburst in a close, clearly interacting companion is a good surrogate for an age determined from the QSO host galaxy itself for purposes of attempting to define an evolutionary sequence.

The AO imaging observations would not have been possible without the support of François

Roddier, Malcolm Northcott, and J. Elon Graves. The AO system used in these observations was built with the support of NSF grant AST93-19004. We thank Jeff Goldader for helpful comments on the spectral synthesis models. This research was partially supported by NSF under grant AST95-29078.

## REFERENCES

- Bruzual, G. & Charlot, S. 1993, *ApJ*, 405, 538
- Bruzual, G. & Charlot, S. 1998, in preparation
- Casali, M. M., & Hawarden, T. G. 1992, *JCMT—UKIRT Newsletter*, No. 3, 33
- Canalizo, G., & Stockton, A. 1998, in preparation
- Canalizo, G., & Stockton, A. 1997, *ApJ*, 480, L5
- Duc, P.-A., & Mirabel, I. F. 1994, *A&A*, 289, 83
- Gunn, J. E., & Stryker, L. L. 1983, *ApJS*, 52, 121
- Hines, D. C., Low, F. J., Thompson, R. J., Weymann, R. J., & Storrie-Lombardi, L. 1998, *BAAS*, 30, in press
- Hodapp, K.-W., et al. 1996, *New Astronomy*, 1, 177
- Hook, R. N., Lucy, L. B., Stockton, A., & Ridgway, S. E. 1994, *ST-ECF Newsletter*, 21, 16
- Hunsberger, S. D., Charlton, J. C., & Zaritsky, D. 1996, *ApJ*, 462, 50
- Hutchings, J. B., & Neff, S. G. 1992, *AJ*, 104, 1
- Hutchings, J. B., Neff, S. G., & Gower, A. C. 1992, *PASP*, 104, 62
- Jacoby, G. H., Hunter, D. A., & Christian, C. A. 1984, *ApJS*, 56, 278
- Mihos, J. C., & Hernquist, L. 1996, *ApJ*, 464, 641
- Roddier, F., Northcott, M. J., & Graves, J. E. 1991, *PASP*, 103, 131
- Roddier, F., Anuskiewicz, J., Graves, J. E., Northcott, M., & Roddier, C. 1994, *Proc. SPIE*, 2201, 2
- Stickel, M., Fried, J. W., McLeod, K. K., & Rieke, G. H. 1995 *AJ*, 109, 1979
- Stockton, A. 1998, in *Galaxy Interactions at Low and High Redshift*, IAU Symp. 186, ed. J. Barnes & D. Sanders, Kluwer, Dordrecht, in press
- Stockton, A., Ridgway, S. E., & Kellogg, M. 1998, in preparation
- Witt, A. N., Thronson, H. A., & Capuano, J. M. 1992, *ApJ*, 393, 611



Fig. 1.— Images of PG 1700+518 obtained with the Canada-France-Hawaii Telescope and the University of Hawaii Adaptive-Optics System. The left-hand column shows different versions of the  $J$ -band image, and the right-hand column shows corresponding versions of the  $H$ -band image. The top row shows the unaltered images of the QSO and nebulosity. The middle row shows PSF-subtracted versions, where the PSF model has been derived from the QSO itself. Any elliptically-symmetric structure in the QSO host galaxy will be subtracted. The bottom row shows *plucy* deconvolutions (Hook *et al.*1994; see text for details), using the same PSF model as the deconvolution kernel. North is up; East to the left.

Fig. 2.— Optical images of PG 1700+518 obtained with the University of Hawaii 88-inch Telescope. The filter central wavelengths are given in the upper-left corner of each panel. In each case, a PSF has been slightly oversubtracted in order to show the extensions clearly (the dark region in the center is the result of saturation in the PSF star, and the vertical streak below the QSO position is a CCD artifact). The insets in the upper left show the images prior to subtraction at the same contrast as the main panel, and those in the lower right show lower-contrast versions of the subtracted images.

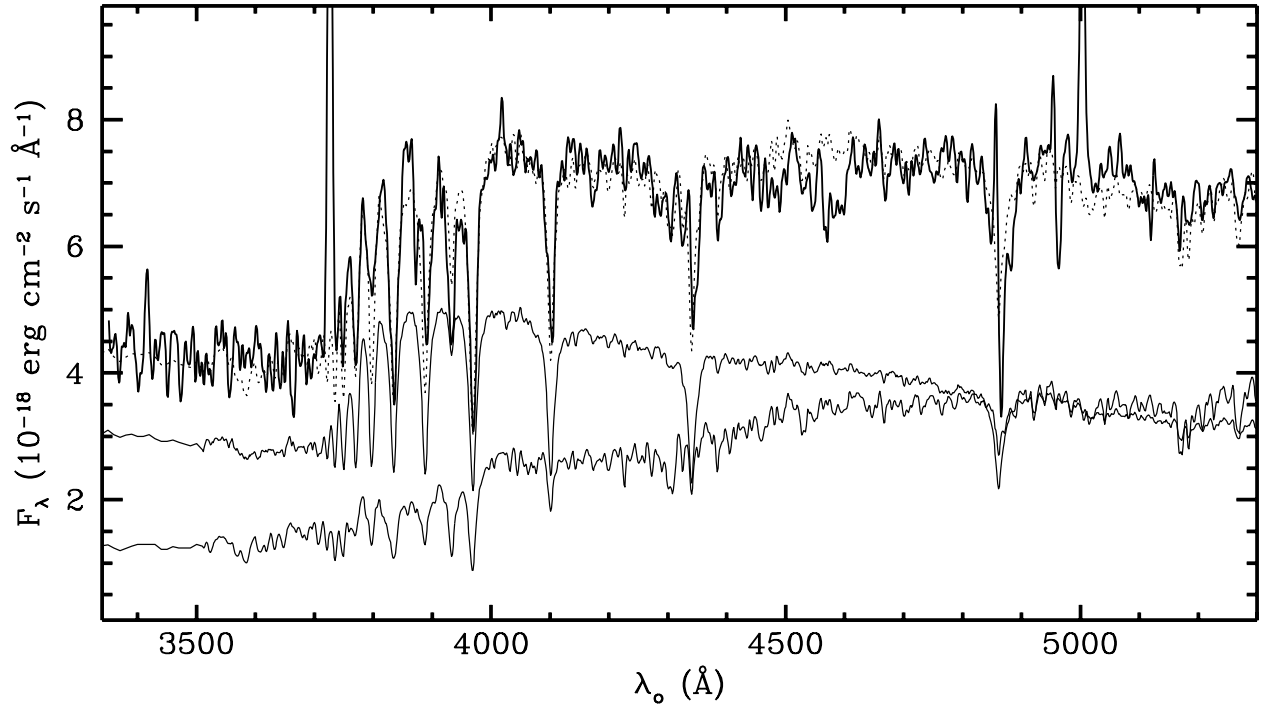


Fig. 3.— Keck LRIS spectrum of the companion  $\sim 2''$  N of PG 1700+518 (heavy line; see Paper 1 for details). The dotted line is the best-fit composite model, comprising an 85 Myr instantaneous burst (upper light line) and an exponentially decreasing star-formation model with a maximum age of 10 Gyr and a time constant of 5 Gyr (lower light line). Both components are multiplied by a reddening curve derived from an embedded-dust model, as described in the text. The apparent [O II]  $\lambda 3727$  and [O III]  $\lambda 5007$  emission lines are not intrinsic to the companion, but are due to general extended emission around the QSO. Weaker, but significant, emission is also present at  $H\beta$ ,  $H\gamma$ , [Ne III]  $\lambda 3868$ , and [O III]  $\lambda 4959$ . Similar emission (but with a higher velocity) in the region used to subtract scattered light from the QSO distorts the  $H\beta$  and  $H\gamma$  absorption profiles (these negative residuals have been corrected for the strong [O II] and [O III] lines).

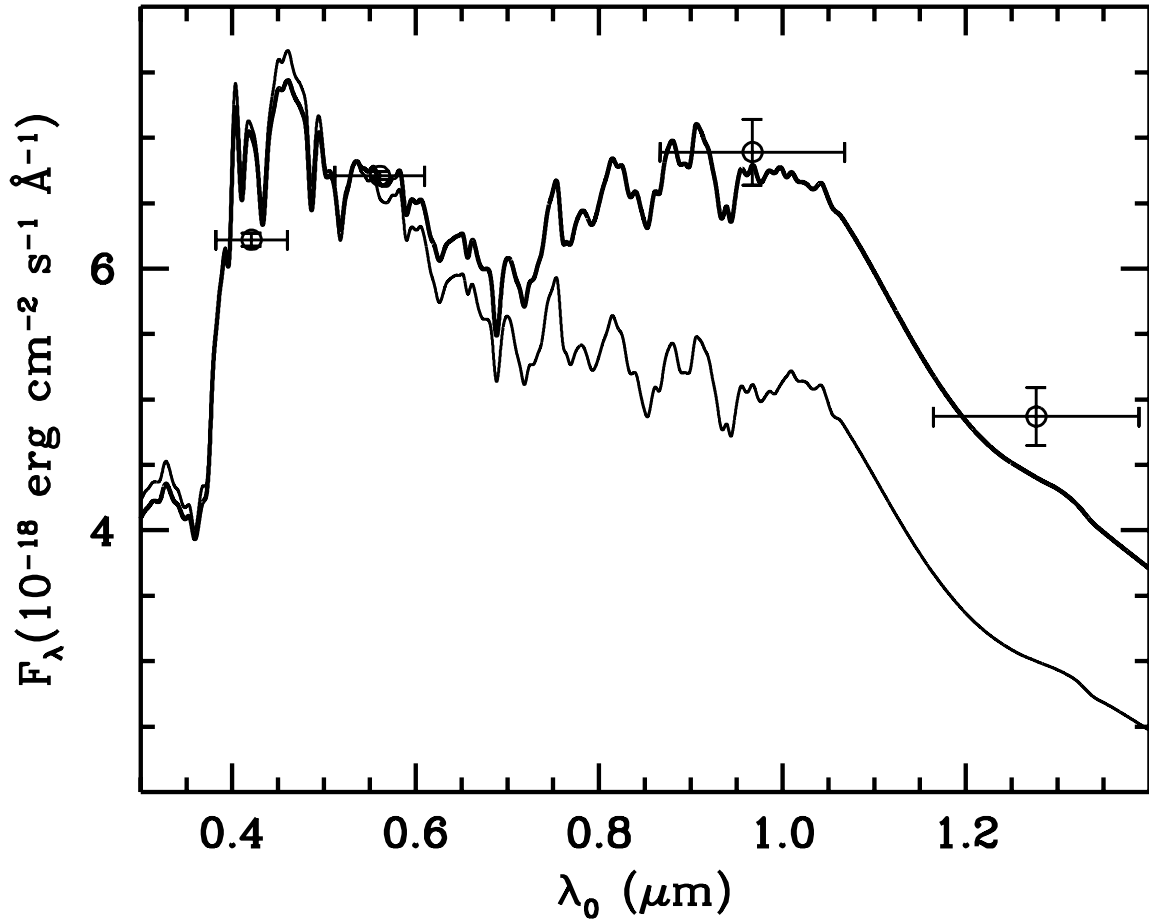


Fig. 4.— Photometry of the PG 1700+518 companion galaxy. The lighter trace shows a model SED comprising instantaneous bursts with ages of 0.114 and 10 Gyrs, and the heavier trace shows the same model as is shown in Fig. 3, renormalized to fit the photometric data.

This figure "fig1.gif" is available in "gif" format from:

<http://arxiv.org/ps/astro-ph/9803333v1>

This figure "fig2.gif" is available in "gif" format from:

<http://arxiv.org/ps/astro-ph/9803333v1>